Neutral Oligosaccharide Structures Linked to Asparagines of Porcine Zona Pellucida Glycoproteins†

Etsuko Mori,‡ Seiichi Takasaki,§ Jerry L. Hedrick,∥ Nate J. Wardrip,∥ Tsuneatsu Mori,‡ and Akira Kobata*,§

Department of Immunology and Biochemistry, Institute of Medical Science, University of Tokyo, Minato-ku, Tokyo 108, Japan, and Department of Biochemistry and Biophysics, University of California, 15 Briggs Hall, Davis, California 95616

Received October 8, 1990

ABSTRACT: N-Linked sugar chains were liberated by hydrazinolysis from porcine zona pellucida glycoproteins obtained from ovarian follicular oocytes. Neutral sugar chains were separated from acidic ones by paper electrophoresis and fractionated with a serial lectin column chromatography and Bio-Gel P-4 column chromatography. Their structural analysis by sequential glycosidase digestion in combination with methylation analysis revealed that the neutral sugar chains are of bi-, tri-, and tetraantennary complex type with a fucosylated trimannosyl core. Twenty-six percent of the sugar chains contain *N*-acetyllactosamine repeating structures in their outer chain moieties. Only linear *N*-acetyllactosamine repeats, the maximum size of which is hexasaccharide, are detected. A characteristic feature is that 39% of the sugar chains contain *N*-acetylglucosamine residues at their nonreducing termini in spite of the absence of bisected sugar chains. This study provided, for the first time, the substantial information about the sugar chain structures of mammalian zona pellucida glycoproteins.

Zona pellucida (ZP)[1] is an extracellular matrix synthesized in and secreted from the mammalian oocytes in developing follicles (Shimizu et al., 1983). It remains around the oocyte after fertilization until the stage of blastocyst (Stambaugh, 1978). It has been proposed that ZP plays important roles in fertilization including species-specific recognition by sperm, prevention of polyspermy, and protection of fertilized eggs (Gwatkin, 1977; Wassarman et al., 1985).

In mice, ZP is reported to be composed of three glycoproteins, ZP1, ZP2, and ZP3, with apparent average molecular sizes of 200, 120, and 83 kDa, which are associated with each other to construct a specific structure (Bleil & Wassarman, 1980b). So far, it has been shown in mice that the mucin-type sugar chains containing α-galactosyl residues in ZP3 work as sperm receptor (Bleil & Wassarman, 1980a, 1988; Florman & Wassarman, 1985) and that the galactosyl transferase on sperm plasma membrane mediates sperm egg binding by interacting with its substrate on zona pellucida (Shur & Hall, 1982; Lopez et al., 1985; Shur & Neely, 1988). In spite of these works suggesting the involvement of sugar moieties of zona pellucida in the receptor activity for sperm, no direct structural analysis of the sugar moieties of ZP glycoproteins has been reported until now. Recent works have shown that porcine oocytes are a more convenient source for structural study because relatively large amounts of the ZP can be obtained. Porcine ZP is also composed of three glycoproteins, one with a molecular size of 82 kDa and the other two with a molecular size of 55 kDa (Hedrick & Wardrip, 1987; Yurewicz et al., 1987). Although the difference in size between porcine and mouse ZP glycoproteins is found, their structural similarity has been shown by using an immunological technique (Kohyama et al., 1985) and a cDNA hybridization technique (Ringuette et al., 1986). A large-scale isolation method of ZP from porcine ovaries has been established (Dumbar et al., 1980; Noda et al., 1981). The previous sugar composition analysis suggested the presence of N- and O-linked sugar chains in porcine ZP glycoproteins (Yurewicz et al., 1987). In this study, the structures of the N-linked, neutral sugar chains were analyzed in detail as a first step to elucidate the roles of the sugar moiety in fertilization.

Materials and Methods

Chemicals, Enzymes, and Lectins. NaB^3H_4 (340 mCi/mmol) and NaB^2H_4 were purchased from New England Nuclear, Boston, MA, and Nacalai Tesque Ltd., Kyoto, respectively. β-Galactosidase, β-*N*-acetylhexosaminidase, and α-mannosidase were purified from jack bean meal by the method of Li and Li (1982). Diplococcal β-galactosidase and β-*N*-acetylhexosaminidase were purified from the culture fluid of *Diplococcus pneumoniae* according to the method of Glasgow et al. (1977). Endo-β-galactosidase from *Flavobacterium keratolyticus* (Kitamikado et al., 1982) and α-mannosidase II from *Aspergillus saitoi* (Amano & Kobata, 1986) were purified according to the cited references. *Aleuria aurantia* lectin (AAL)–Sepharose (Yazawa et al., 1984) and *Datura stramonium* agglutinin (DSA)–Sepharose (Yamashita et al., 1987) were prepared according to the cited references, respectively. Concanavalin A (Con A)–Sepharose was purchased from Pharmacia, Uppsala.

Analytical Methods. Glycosidase digestions were carried out as described previously (Yoshima et al., 1980; Mizoguchi et al., 1984). Paper electrophoresis (Takasaki et al., 1984), Bio-Gel P-4 (minus 400 mesh) column chromatography (Yamashita et al., 1982), and affinity chromatography on AAL–Sepharose (Yamashita et al., 1985) and DSA–Sepharose (Yamashita et al., 1987) were performed according to the cited references. Con A–Sepharose column chromatography was performed as described by Cummings and Kornfeld (1982), except that 5 mM methyl α-glucoside, instead of 10

† This work was supported by the Grant-in-Aid for Priority Area "Germ Line" from the Ministry of Education, Science and Culture of Japan.

* Address correspondence to this author.
‡ Department of Immunology, University of Tokyo.
§ Department of Biochemistry, University of Tokyo.
∥ University of California.

[1] Abbreviations: ZP, zona pellucida; AAL, *Aleuria aurantia* lectin; Con A, concanavalin A; DSA, *Datura stramonium* agglutinin.

0006-2960/91/0430-2078$02.50/0

mM, was used. Methylation analysis of oligosaccharides was performed as described previously (Kagawa et al., 1988). Paper chromatography was carried out by using either of the two solvent systems: solvent I, 1-butanol/ethanol/water (4:1:1 v/v); solvent II, ethyl acetate/pyridine/acetic acid/water (5:5:1:3 v/v).

Preparation of ZP Glycoproteins. ZP glycoproteins were isolated from frozen porcine ovaries according to the procedure described previously (Dumbar et al., 1980). The procedure includes separation of oocytes from ovaries, isolation of the ZP from homogenized oocytes, and solubilization of ZP glycoproteins.

Release of the Asparagine-Linked Sugar Chains as Oligosaccharides from ZP Glycoproteins. Twenty milligrams of ZP glycoproteins was subjected to hydrazinolysis as described previously (Takasaki et al., 1982). The oligosaccharide fraction was freed from contaminating peptide components by paper chromatography using solvent II. One-fourth of the oligosaccharide fraction was reduced with NaB^3H_4 to obtain a tritium-labeled oligosaccharide mixture. The remaining three-fourths of oligosaccharide fraction was reduced with NaB^2H_4 and provided for methylation analysis.

Oligosaccharides. Galβ1→4GlcNAcβ1→6(Galβ1→4GlcNAcβ1→2)Manα1→6[Galβ1→4GlcNAcβ1→4(Galβ1→4GlcNAcβ1→2)Manα1→3]Manβ1→4GlcNAcβ1→4(Fucα1→6)GlcNAc$_{OT}$[2] (Gal_4·GlcNAc$_4$·Man_3·GlcNAc·Fuc·GlcNac$_{OT}$), Galβ1→4GlcNAcβ1→6(Galβ1→4GlcNAcβ1→2)Manα1→6(Galβ1→4GlcNAcβ1→2Manα1→3)Manβ1→4GlcNAcβ1→4(Fucα1→6)GlcNAc$_{OT}$ (2,6-branched Gal_3·$GlcNAc_3$·Man_3·GlcNAc·Fuc·GlcNAc$_{OT}$), Galβ1→4GlcNAcβ1→2Manα1→6[Galβ1→4GlcNAcβ1→4(Galβ1→4GlcNAcβ1→2)Manα1→3]Manβ1→4GlcNAcβ1→4(Fucα1→6)GlcNAc$_{OT}$(2,4-branched Gal_3·$GlcNAc_3$·Man_3·GlcNAc·Fuc·GlcNAc$_{OT}$), and Galβ1→4GlcNAcβ1→2Manα1→6(Galβ1→4GlcNAcβ1→2Manα1→3)Manβ1→4GlcNAcβ1→4(Fucα1→6)GlcNAc$_{OT}$ (Gal_2·$GlcNAc_2$·Man_3·GlcNAc·Fuc·GlcNAc$_{OT}$) were obtained from recombinant human erythropoietin by hydrazinolysis (Takeuchi et al., 1988). Manα1→6(3)[Galβ1→4GlcNAcβ1→2Manα1→3(6)]Manβ1→4GlcNAcβ1→(Fucα1→6) GlcNAc$_{OT}$ (Gal·GlcNAc·Man_3·GlcNAc·Fuc·GlcNAc$_{OT}$) was prepared from hamster melanoma tyrosinase (Ohkura et al., 1984). Degalactosylated oligosaccharides were prepared by jack bean β-galactosidase digestion of the oligosaccharides described above. Manα1→6(Manα1→3)Manβ1→4GlcNAcβ1→4(Fucα1→6)GlcNAc$_{OT}$ (Man_3·GlcNAc·Fuc·GlcNAc$_{OT}$) was obtained by digestion of Gal_2·$GlcNAc_2Man_3$·GlcNAc·Fuc·GlcNAc$_{OT}$ with a mixture of diplococcal β-galactosidase and diplococcal β-*N*-acetylhexosaminidase.

Results

Fractionation of Oligosaccharides Released from ZP Glycoproteins. The radioactive oligosaccharide mixture, obtained from ZP glycoproteins by hydrazinolysis, was subjected to paper electrophoresis at pH 5.4. As shown in Figure 1, the sample was separated into a neutral fraction (N) and an extremely heterogeneous acidic fraction (A) in a percent molar ratio of 33 to 67. The fraction N was then subjected to serial lectin column chromatography (Figure 2). The sample was first applied to a column of AAL–Sepharose to separate into the passed-through fraction (AAL^-) and the bound fraction (AAL^+), which was eluted from the column with the buffer containing 1 mM fucose. Only 3% of fraction N was recovered

[2] Subscript OT indicates NaB^3H_4-reduced oligosaccharides.

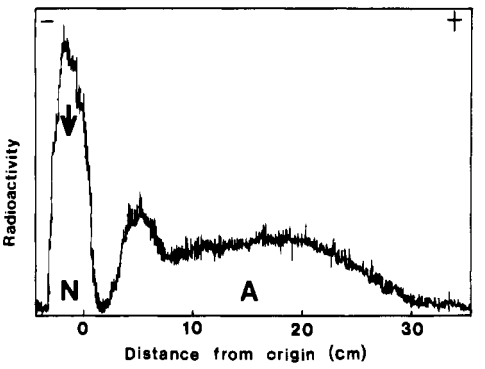

FIGURE 1: Paper electrophoresis of the radioactive oligosaccharides obtained from porcine ZP glycoproteins. The oligosaccharides released from ZP glycoproteins by hydrazinolysis were subjected to paper electrophoresis at pH 5.4 (73 V/cm, 90 min). The arrow indicates the position of neutral oligosaccharides.

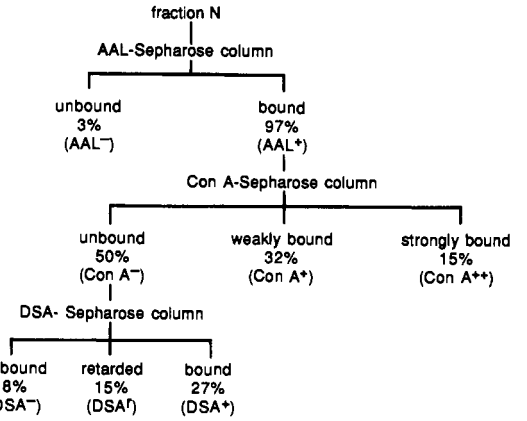

FIGURE 2: Fractionation of the neutral oligosaccharides by serial immobilized lectin column chromatography. The radioactive fraction N in Figure 1 was first subjected to AAL–Sepharose column chromatography. The fraction bound to the column (AAL^+) was then applied to a column of Con A–Sepharose. The fraction passed through the Con A–Sepharose column ($Con\ A^-$) was subjected to DSA–Sepharose column chromatography. The numbers indicate the percent molar ratios of each fraction to the total neutral oligosaccharides.

in the AAL^- fraction, and the remainder was in the AAL^+ fraction, indicating that almost all of the neutral oligosaccharides contain α-fucose residues. When the AAL^- fraction was applied to a Con A–Sepharose column, it completely passed through the column. No further analysis of this fraction was performed because of the limited amount of the sample available. However, this chromatographic behavior indicates that high mannose type oligosaccharides known to interact strongly with Con A are not included in porcine ZP.

By Con A–Sepharose column chromatography, the AAL^+ fraction was separated into three fractions; the passed-through fraction ($Con\ A^-$) and the bound fractions eluted with 5 mM methyl α-glucoside ($Con\ A^+$) and then with 100 mM methyl α-mannoside ($Con\ A^{++}$). The AAL^+ $Con\ A^-$ fraction thus obtained was further applied to a DSA–Sepharose column and separated into the passed-through fraction (DSA^-), the retarded fraction (DSA^r), and the bound fraction (DSA^+) which was eluted with the buffer containing 1% *N*-acetylglucosamine oligomers. The series of lectin column chromatography was summarized in Figure 2 together with the percent molar ratio of each fraction to the total neutral oligosaccharides. Five fractions except for AAL^- $Con\ A^-$ fraction were shown to contain multiple components by Bio-Gel P-4 column chromatography (Figure 3).

Methylation Analysis and Preliminary Structural Studies of Oligosaccharides in Fraction AAL^+. Because of the limited

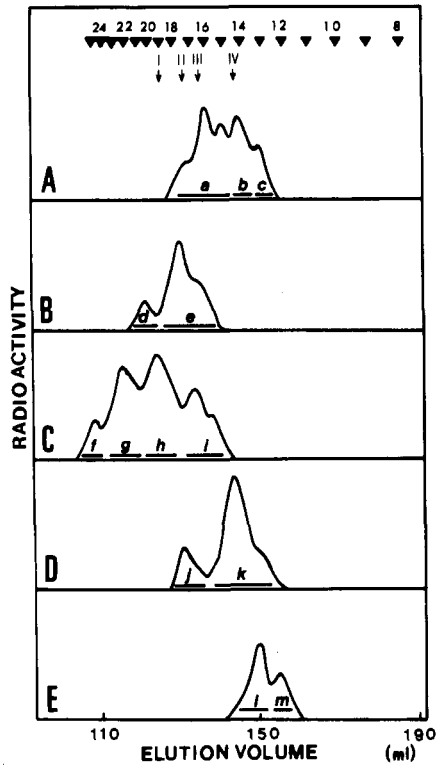

FIGURE 3: Bio-Gel P-4 column chromatography of the oligosaccharides fractionated by serial lectin column chromatography. Fractions DSA^- (panel A), DSA^r (panel B), DSA^+ (panel C), Con A^+ (panel D), and Con A^{++} (panel E) were applied to a column of Bio-Gel P-4. Arrows I, II, III, and IV indicate the elution positions of authentic Gal_4·$GlcNAc_4$·Man_3·GlcNAc·Fuc·$GlcNAc_{OT}$, 2,4-branched Gal_3·$GlcNAc_3$·Man_3·GlcNAc·Fuc·$GlcNAc_{OT}$, 2,6-branched Gal_3·$GlcNAc_3$·Man_3·GlcNAc·Fuc·$GlcNAc_{OT}$, and Gal_2·$GlcNAc_2$·Man_3·GlcNAc·Fuc·$GlcNAc_{OT}$, respectively. Black arrowheads indicate the elution positions of glucose oligomers, and the numbers indicate the glucose units.

Table I: Methylation Analysis of AAL^+ Fraction

methylated sugar	molar ratio[a]
fucitols	
2,3,4-tri-*O*-methyl (1,5-di-*O*-acetyl)	0.8
galactitols	
2,3,4,6-tetra-*O*-methyl (1,5-di-*O*-acetyl)	2.4
2,4,6-tri-*O*-methyl (1,3,5-tri-*O*-acetyl)	0.6
mannitols	
3,4,6-tri-*O*-methyl (1,2,5-tri-*O*-acetyl)	1.1
3,6-di-*O*-methyl (1,2,4,5-tetra-*O*-acetyl)	0.4
3,4-di-*O*-methyl (1,2,5,6-tetra-*O*-acetyl)	0.3
2,4-di-*O*-methyl (1,3,5,6-tetra-*O*-acetyl)	1.0
2-(*N*-methylacetamido)-2-deoxyglucitols	
3,6-di-*O*-methyl (1,4,5-tri-*O*-acetyl)	3.1
1,3,5-tri-*O*-methyl (4,6-di-*O*-acetyl)	0.9
3.4.6-tri-*O*-methyl (1,5-di-*O*-acetyl)	0.8

[a] Numbers were calculated by taking the value of 2,4-di-*O*-methylmannitol as 1.0.

amount of the sample available and the heterogeneous nature of the oligosaccharides (Figure 3), methylation analysis of only the AAL^+ fraction was performed to obtain the outline of the glycosidic linkages included in the oligosaccharides in this fraction. The results are summarized in Table I.

All fucose residues occur at nonreducing termini. Detection of 3,4,6-tri-, 3,6-di-, 3,4-di-, and 2,4-di-*O*-methylmannitols indicates that mannose residues occur in four forms: $\rightarrow 2Man1\rightarrow$, $\rightarrow^{4}_{2}Man1\rightarrow$, $\rightarrow^{6}_{2}Man1\rightarrow$, and $\rightarrow^{6}_{3}Man1\rightarrow$. Detection of 1,3,5-tri-*O*-methyl 2-(*N*-methylacetamido)-2-deoxyglucitol but not the 1,3,5,6-tetra-*O*-methyl derivative indicates that the *N*-acetylglucosaminitol at reducing termini occurs

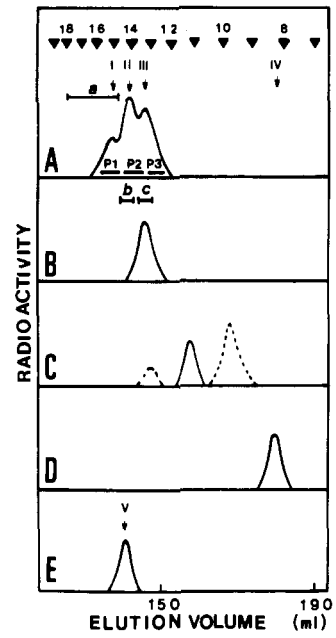

FIGURE 4: Sequential glycosidase digestion of oligosaccharides in the DSA^- fraction. Fraction a in Figure 3A was digested with diplococcal β-galactosidase (panel A). Fractions b and c in Figure 3A were also digested with diplococcal β-galactosidase (panel B). Radioactive peaks P1, P2, and P3 in panel A were separately digested with diplococcal β-*N*-acetylhexosaminidase (panel C): dashed line, dotted line, and solid line in panel C indicate the products from P1, P2, and P3, respectively. The peaks in panel C were then digested with jack bean β-*N*-acetylhexosaminidase (panel D). Fraction a was also digested with jack bean β-*N*-acetylhexosaminidase (panel E). Arrows indicate the elution positions of authentic oligosaccharides: I, $GlcNAc_4$·Man_3·GlcNAc·Fuc·$GlcNAc_{OT}$; II, 2,4-branched $GlcNAc_3$·Man_3·GlcNAc·Fuc·$GlcNAc_{OT}$; III, 2,6-branched $GlcNAc_3$·Man_6·GlcNAc·Fuc·$GlcNAc_{OT}$; IV, Man_3·GlcNAc·Fuc·$GlcNAc_{OT}$; V, Gal_2·$GlcNAc_2$·Man_3·GlcNAc·Fuc·$GlcNAc_{OT}$. Black arrowheads are the same as in Figure 3. Bars a in panel A and b and c in panel B indicate the elution positions of fractions a, b, and c, respectively (see also Figure 3A).

exclusively as $\rightarrow^{6}_{4}GlcNAc_{OT}$. When digested with a mixture of diplococcal β-galactosidase and jack bean β-*N*-acetylhexosaminidase, the radioactive oligosaccharide mixture in the AAL^+ fraction was all converted to the fucosylated trimannosyl core, Manα1→6(Manα1→3)Manβ1→4GlcNAcβ1→4(Fucα1→6)$GlcNAc_{OT}$ (data not shown). These results indicate that the AAL^+ fraction is composed of complex-type oligosaccharides which do not contain any fucose residue in the outer chain moieties but do in the trimannosyl cores. In addition, the absence of 2-mono-*O*-methylmannitol indicates that no bisected oligosaccharide is included. Therefore, the molar ratio of each methylated sugar was calculated by taking the value of 2,4-di-*O*-methylmannitol as 1.0.

N-Acetylglucosamine residues except for those at reducing termini were detected as 3,6-di- and 3,4,6-tri-*O*-methyl 2-(*N*-methylacetamido)-2-deoxyglucitols, indicating that these residues occur in two forms, →4GlcNAc1→ and GlcNAc1→. This result indicates that some of the outer chains might be terminated with *N*-acetylglucosamine residues. Detection of small amount of 2,4,6-tri-*O*-methylgalactitol in addition to 2,3,4,6-tetra-*O*-methylgalactitol suggests the occurrence of an *N*-acetyllactosamine repeat. To characterize the structures of repeating units, an aliquot of the deuterium-labeled neutral oligosaccharide mixture was digested with endo-β-galactosidase and labeled with NaB^3H_4. When applied to a Bio-Gel P-4 column, two radioactive components with 4.5 and 3.5 glucose units were obtained in the molar ratio of 3 to 2 (data not

shown). These two components were identified as Galβ1→4GlcNAcβ1→Gal_{OT} and GlcNAcβ1→Gal_{OT} by sequential digestion with diplococcal β-glactosidase and jack bean β-*N*-acetylhexosaminidase. Thus, the occurrence of linear *N*-acetyllactosamine repeating units was verified.

By taking these results into consideration, neutral oligosaccharides in the AAL^+ fraction are considered to have the following generalized structures:

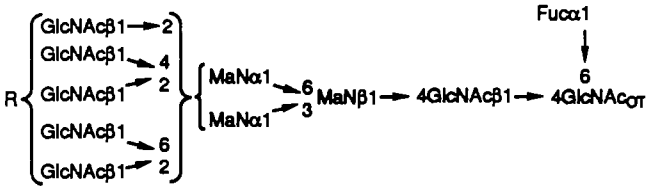

in which R represents ±Galβ1→4 or ±Galβ1→4-(GlcNAcβ1→3Galβ1→4)$_n$.

Structural Analysis of Oligosaccharides in the DSA⁻ Fraction. Fractions a–c in Figure 3A were subjected to sequential exoglycosidase digestion. When incubated with diplococcal β-galactosidase, fraction a produced three radioactive peaks, P1, P2, and P3 as shown in Figure 4A, while fraction b was converted to a peak with the same elution position as P3 with release of one galactose residue (Figure 4B) Fraction c, which was eluted at the same position as P3, was resistant to the diplococcal β-galactosidase digestion (Figure 4B). The structues of P1, P2, and P3 are proposed as shown by the following experiments:

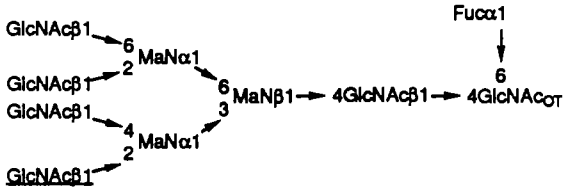

P1

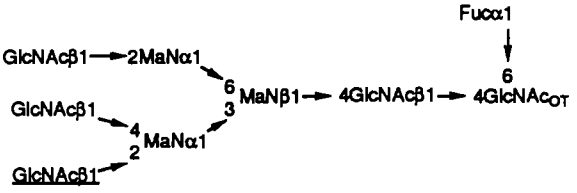

P2

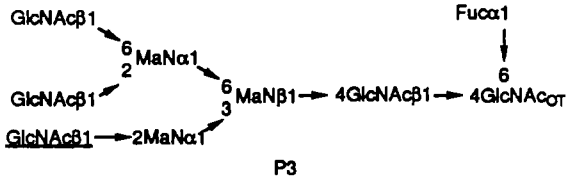

P3

Diplococcal β-*N*-acetylhexosaminidase is well-known to cleave GlcNAcβ1→2 linkages in the GlcNAcβ1→2Man group and the GlcNAcβ1→4(GlcNAcβ1→2)Man group but not in the GlcNAcβ1→6(GlcNAcβ1→2)Man group (Yamashita et al., 1981). Therefore, *N*-acetylglucosamine residues underlined in the proposed structures should be removed by this enzyme. Actually, the digestion released one residue of *N*-acetylglucosamine from P1 (Figure 4C, dashed line), two residues from P2 (Figure 4C, dotted line), and one residue from P3 (Figure 4C, solid line), respectively. The remaining three, one, and two *N*-acetylglucosamine residues in P1, and P2, and P3, respectively, were all released by jack bean β-*N*-acetylhexosaminidase digestion, and fucosylated trimannosyl core, Man_3·GlcNAc·Fuc·$GlcNAc_{OT}$, was obtained (Figure 4D). Upon digestion with *A. saitoi* α-mannosidase II, which cleaves the α-mannosyl linkage of R→Manα1→6(Manα1→3)-Manβ1→4R′ but not of Manα1→6(R→Manα1→3)-Manβ1→4R′ (Amano & Kobata, 1986), one mannose residue was removed from the solid line peak in Figure 4C, but not from the dotted line peak in Figure 4C (data not shown). Therefore, it is proposed that 2,6-branching is exclusively located on the Manα1→6 arm and 2,4-branching on the Manα1→3 arm, respectively.

On the basis of these results, fraction a was suppossed to be a mixture of tetraantennary oligosaccharides and 2,4- and 2,6-branched triantennary oligosaccharides which are partly galactosylated. Numbers of galactose residues in these oligosaccharides were examined as follows. When fraction a was digested with jack bean β-*N*-acetylhexosaminidase, a single radioactive peak with the same elution position as authentic Gal_2·$GlcNAc_2$·Man_3·GlcNAc·Fuc·$GlcNAc_{OT}$ was obtained (Figure 4E). This radioactive component was converted to Man_3·GlcNAc·Fuc·$GlcNAc_{OT}$ by sequential digestion with jack bean β-galactosidase and β-*N*-acetylhexosaminidase, releasing 2 mol each of galactose and *N*-acetylglucosamine residues (data not shown). These results indicated that all oligosaccharides in fraction a contain two Galβ1→ groups in their outer chain moieties. Since fraction a passed through a DSA–Sepharose column which requires the Galβ1→4GlcNAcβ1→4(Galβ1→4GlcNAcβ1→2)Man group for retardation and the Galβ1→4GlcNAcβ1→6(Galβ1→4GlcNAcβ1→2)Man group for binding (Cummings & Kornfeld, 1984; Yamashita et al., 1987), the two Galβ1→4GlcNAcβ1→ groups should not be linked to the same α-mannosyl residue of the fucosylated trimannosyl core. Considering these results, the structures of three oligosaccharides, a1, a2, and a3, in fraction a are proposed as shown in Table II.

The degalactosylated fractions b and c, the peak in Figure 4B, were proven to be identical with P3 in Figure 4A by the same sequential glycosidase digestion as indicated by solid lines in Figure 4C,D. Therefore, the structures of fractions b and c are proposed as shown in Table II.

Structural Analysis of Oligosaccharides in DSA′ Fraction. Upon digestion with endo-β-galactosidase, the effective size of fraction d in Figure 3B was decreased by three glucose units (Figure 5A), indicating that one GlcNAc·Gal group was removed. Since this product was also retarded from a DSA–Sepharose column, a Galβ1→4GlcNAcβ1→4(Galβ1→4GlcNAcβ1→2)Man group should be left intact after the enzymatic digestion (Yamashita et al., 1987). The product was digested with diplococcal β-galactosidase with release of two galactose residues, producing a radioactive component eluting at the position corresponding to authentic $GlcNAc_4$·Man_3·GlcNAc·Fuc·$GlcNAc_{OT}$ (Figure 5B). That the peak in Figure 5B is identical with oligosaccharide P1 in Figure 4A was confirmed by the series of analyses already described for P1. When fraction d was digested with jack bean β-*N*-acetylhexosaminidase, two *N*-acetylhexosamine residues were removed (Figure 5C). These results indicate that the component in fraction d is tetraantennary oligosaccharides, the 2,6-branching of which gives GlcNAcβ1→3Galβ1→4GlcNAcβ1→ and GlcNAcβ1→ as shown in Table II.

Fraction e in Figure 3B was mainly eluted at the same position as authentic 2,4-branched Gal_3·$GlcNAc_3$·Man_3·GlcNAc·Fuc·$GlcNAc_{OT}$. The elution pattern showed that a minor component which is smaller than the major peak by one glucose unit is included in this fraction. With release of three and two galactose residues, respectively, from the major peak

Table II: Proposed Structures of Oligosaccharides Obtained from ZP Glycoproteins

structures	molar ratio (%)	fraction
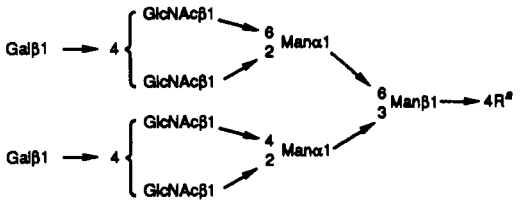	0.8	a1
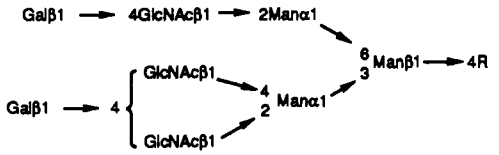	2.9	a2
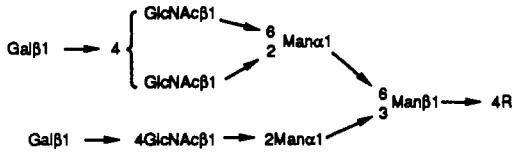	1.4	a3
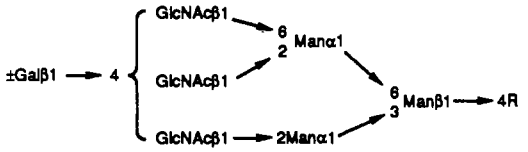	(+) 1.8 (−) 1.1	b c
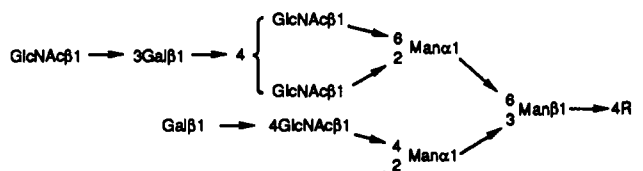	1.4	d
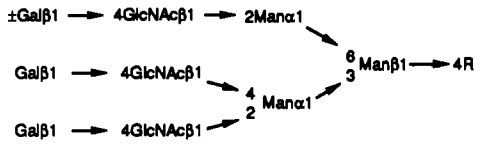	(+) 10.7 (−) 2.9	e1 e2
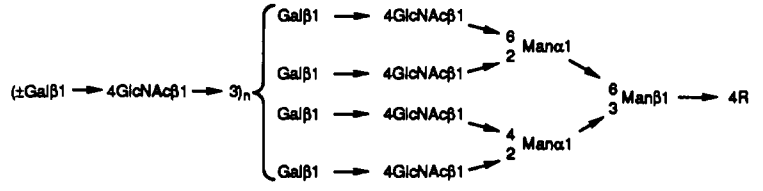	(n = 2)[b] 0.8 (n = 1) 3.7 (n = 0) 3.5	f1 g1 h1
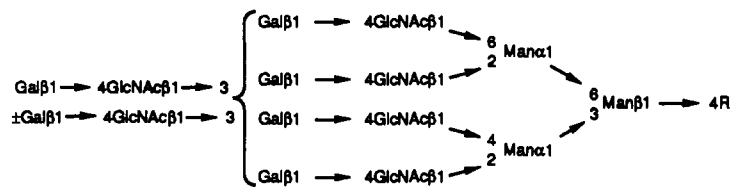	1.9	f2
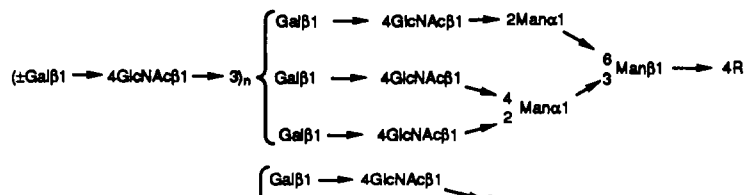	(n = 2)[b] 2.3 (n = 1) 5.3	g2 h2
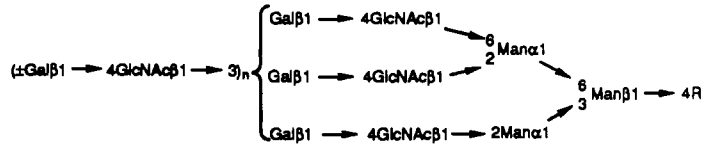	(n = 2)[b] 2.7 (n = 1) 1.7	g3 h3

Table II (Continued)

structures	molar ratio (%)	fraction
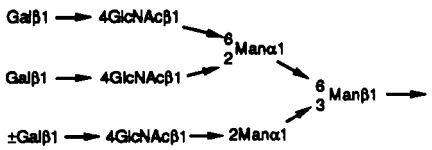	(+) 3.4 (−) 1.7	i1 i2
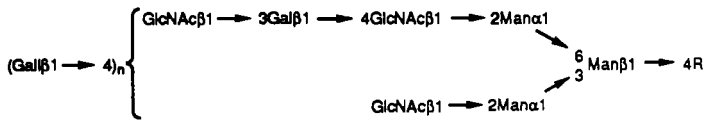	(*n* = 2) 5.1 (*n* = 1) 0.8	j1 j2
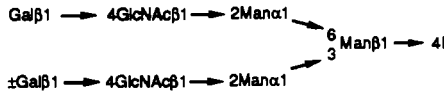	(+) 22.8 (−) 3.3	k1 k2
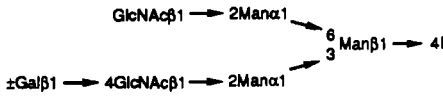	(+) 11.6 (−) 3.4	l m

[a] R represents GlcNAcβ1→4(Fucα1→6)GlcNAc$_{OT}$. [b] The ±Galβ1→4GlcNAcβ1→3Galβ1→4GlcNAcβ1→3 sequence is indicated by (±Galβ1→4GlcNAcβ1→3)$_2$.

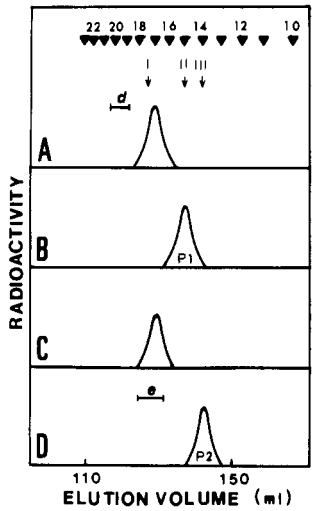

FIGURE 5: Sequential glycosidase digestion of oligosaccharides in DSA^r fraction. Fraction d in Figure 3B was sequentially digested with endo-β-galactosidase (panel A) and diplococcal β-galactosidase (panel B). Fraction d was also digested with jack bean β-*N*-acetylhexosaminidase (panel C). Fraction e in Figure 3B was digested with diplococcal β-galactosidase (panel D). Arrows indicate the elution positions of authentic oligosaccharides: I, 2,4-branched Gal_3·$GlcNAc_3$·Man_3·GlcNAc·Fuc·GlcNAc$_{OT}$; II, $GlcNAc_4$·Man_3·GlcNAc·Fuc·GlcNAc$_{OT}$; III, 2,4-branched $GlcNAc_3$·Man_3·GlcNAc·Fuc·GlcNAc$_{OT}$. Black arrowheads are the same as in Figure 3. Bars d and e in panel A and D indicate the elution positions of fractions d and e, respectively (see also Figure 3B).

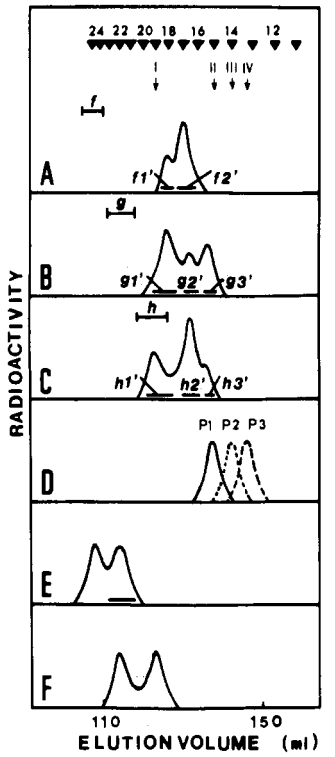

FIGURE 6: Sequential glycosidase digestion of oligosaccharides in the DSA$^+$ fraction. Fractions f (panel A), g (panel B), and h (panel C) in Figure 3C were digested with endo-β-galactosidase, respectively. By diplococcal β-galactosidase digestion, peaks f1′and f2′ in panel A, peak g1′ in panel B, and peak h1′ in panel C were all converted to P1 (panel D, solid line), peak g2′ in panel B and peak h2′ in panel C to P2 (panel D, dotted line), and peak g3′ in panel B and h3′ in panel C to P3 (panel D, dashed line), respectively. Fractions f (panel E) and g (panel F) were also digested with jack bean β-*N*-acetylhexosaminidase, respectively. Arrows indicate the elution positions of authentic oligosaccharides: I, Gal_4·$GlcNAc_4$·Man_3GlcNAc·Fuc·GlcNAc$_{OT}$; II, $GlcNAc_4$·Man_3·GlcNAc·Fuc·GlcNAc$_{OT}$; III, 2,4-branched $GlcNAc_3$·Man_3·GlcNAc·Fuc·GlcNAc$_{OT}$; IV, 2,6-branched $GlcNAc_3$·Man_3·GlcNAc·Fuc·GlcNAc$_{OT}$. Black arrowheads are the same as in Figure 3. Bars f, g, and h in panels A, B, and C, respectively, indicate the elution positions of fractions f, g, and h (see also Figure 3C).

and the minor peak by diplococcal β-galactosidase digestion, fraction e was converted to a radioactive component with the same mobility as authentic 2,4-branched $GlcNAc_3$·Man_3·GlcNAc·Fuc·GlcNAc$_{OT}$ (Figure 5D). That it has the same structure as P2 in Figure 4A was confirmed by the series of analyses already described for P2. Considering these results and the fact that this fraction was retarded in a DSA–Sepharose column, fraction e is proposed to contain two 2,4-branched triantennary oligosaccharides (e1 and e2) as shown in Table II.

Structural Analysis of Oligosaccharides in DSA$^+$ Fraction. When fraction f was digested with endo-β-galactosidase, it was converted to two radioactive components f1′ and f2′ (Figure 6A). Diplococcal β-galactosidase treatment released two galactose residues from the components f2′ and three from the component f1′ and produced the same radioactive component

P1 (Figure 6D, solid line) which was identified as $GlcNAc_4{\cdot}Man_3{\cdot}GlcNAc{\cdot}Fuc{\cdot}GlcNAc_{OT}$ in the same way as described for component P1 in Figure 4A. Jack bean β-*N*-acetylhexosaminidase digestion released one *N*-acetylglucosamine residue from 53% of fraction f (Figure 6E), indicating that one exposed *N*-acetylglucosamine residue is included in part of the oligosaccharides in this fraction. Therefore, fractions f1′ and f2′ were considered to be produced from the following tetraantennary oligosaccharides f1 and f2 by endo-β-galactosidase digestion:

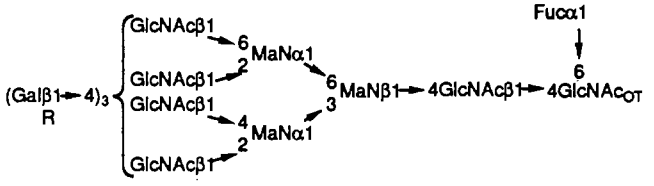

f1: R = ±Galβ1→4GlcNAcβ1→3Galβ1→4GlcNAcβ1→3Galβ1→4

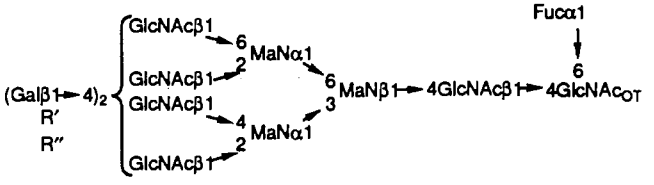

f2: R′ = Galβ1→4GlcNAcβ1→3Galβ1→4; R″ = ±Galβ1→4GlcNAcβ1→3Galβ1→4

That the nonreducing terminal *N*-acetylglucosamine residues are included in some of the repeating units was confirmed by the following experiment. The peak indicated by a bar in Figure 6E should be devoid of exposed *N*-acetylglucosamine residue because it was obtained by exhaustive jack bean β-*N*-acetylhexosaminidase digestion of fraction f. When this peak was digested with endo-β-galactosidase, only one radioactive product with the same effective size as f1′ in Figure 6A, which corresponds to $Gal_3{\cdot}GlcNAc_4{\cdot}Man_3{\cdot}GlcNAc{\cdot}Fuc{\cdot}GlcNAc_{OT}$, was obtained (data not shown). Thus, the result supports that the structures proposed above are correct. On the basis of these results, the structures of oligosaccharides f1 and f2 in fraction f are proposed as shown in Table II.

Endo-β-galactosidase digestion of fraction g produced three radioactive components g1′, g2′, and g3′ (Figure 6B). By diplococcal β-galactosidase digestion components g1′, g2′, and g3′ were converted to the radioactive peaks P1 (solid line), P2 (dotted line), and P3 (dashed line), respectively, with release of three galactose residues from g1′ and two each from g2′ and g3′ (Figure 6D). Subsequent digestion of these peaks P1, P2, and P3 with diplococcal and jack bean β-*N*-acetylhexosaminidase gave the same results as obtained for P1, P2, and P3 in Figure 4A (Figure 4C,D), which were identified as $GlcNAc_4{\cdot}Man_3{\cdot}GlcNAc{\cdot}Fuc{\cdot}GlcNAc_{OT}$ and 2,4-branched and 2,6-branched $GlcNAc_3{\cdot}Man_3{\cdot}GlcNAc{\cdot}Fuc{\cdot}GlcNAc_{OT}$, respectively. When each of g1′, g2′ and g3′ was digested with jack bean β-*N*-acetylhexosaminidase, only one *N*-acetylglucosamine residue newly exposed by endo-β-galactosidase digestion was removed (data not shown). These data indicated that the *N*-acetyllactosamine repeating unit is included at one site each on the outer chains of tetraantennary and two isomeric triantennary oligosaccharides and that the intact oligosaccharides in fraction g contain no exposed *N*-acetylglucosamine residue linked to the trimannosyl cores. However, the occurrence of the nonreducing terminal *N*-acetylglucosamine residue in the *N*-acetyllactosamine repeating unit is suspected, since fraction g was eluted as a peak with a shoulder from a Bio-Gel P-4 column (Figure 3C). Actually, the shoulder disappeared after jack bean β-*N*-acetylhexosaminidase digestion of fraction g, and a smaller sized radioactive peak appeared by removal of one *N*-acetylhexosamine residue (Figure 6F), indicating that 49% of fraction g contains exposed *N*-acetylglucosamine residues in the repeating units. These results indicate that fraction g is composed of tetraantennary oligosaccharides g1 with ±Galβ1→4GlcNAcβ1→3Galβ1→4GlcNAc outer chains and 2,4-branched (g2) and 2,6-branched (g3) triantennary oligosaccharides, both of which contain ±Galβ1→4GlcNAcβ1→3Galβ1→4GlcNAcβ1→3Galβ1→4GlcNAc outer chains (Table II).

After endo-β-galactosidase digestion, fraction h was separated into three components, h1′, h2′, and h3′ (Figure 6C). Component h1′, which was resistant to the enzymatic digestion, was converted to peak P1 with release of four galactose residues by diplococcal β-galactosidase digestion (Figure 6D, solid line). Components h2′ and h3′ gave the same results as components g2′ and g3′, respectively, in a series of glycosidase digestions. Jack bean β-*N*-acetylhexosaminidase digestion did not change the elution position of fraction h (data not shown). From these results and the size difference before and after endo-β-galactosidase digestion, it was concluded that fraction h is composed of typical tetraantennary oligosaccharide (h1) and 2,4-branched (h2) and 2,6-branched (h3) triantennary oligosaccharides containing a Galβ1→4GlcNAcβ1→3Galβ1→4GlcNAc sequence at one site of their outer chain moieties (Table II).

Fraction i was eluted as a major peak with a shoulder (Figure 3C). When digested with diplococcal β-galactosidase, it was converted to the radioactive component P3 with release of three galactose residues from the major peak and two from the shoulder (Figure 6D, dashed line). Since the presence of the Galβ1→4GlcNAcβ1→6(Galβ1→4GlcNAcβ1→2)Man group is required for its binding to DSA–Sepharose column (Cummings & Kornfeld, 1984; Yamashita et al., 1987), fraction i is proposed to contain 2,6-branched triantennary oligosaccharide (i1) and that lacking one galactose residue on the Manα1→3 side (i2) as shown in Table II.

Structural Analysis of Oligosaccharides in the Con A$^+$ and Con A^{++} Fractions. As shown in Figure 3D, fraction j was composed of a major peak with a small shoulder. By diplococcal β-galactosidase digestion, fraction j was converted to a single radioactive component with release of two galactose residues from the major peak and one from the shoulder (Figure 7A). Digestion of this product with diplococcal β-*N*-acetylhexosaminidase yielded a component with the same effective size as authentic $Gal{\cdot}GlcNAc{\cdot}Man_3{\cdot}GlcNAc{\cdot}Fuc{\cdot}GlcNAc_{OT}$ with release of two *N*-acetylglucosamine residues (Figure 7B). This component was then converted to the trimannosyl core by another cycle of sequential digestion with diplococcal β-galactosidase and diplococcal β-*N*-acetylhexosaminidase (Figure 7C). The data indicate that fraction j contains biantennary oligosaccharide with one each of the Galβ1→4GlcNAcβ1→3Galβ1→4GlcNAcβ1→ and the Galβ1→4GlcNAcβ1→ outer chains and its one galactose-less derivative as a minor component. Actually, fraction j was sensitive to endo-β-galactosidase digestion (data not shown). When the peak in Figure 7B was digested with *A. saitoi* α-mannosidase II, one mannose residue was removed (data not shown), indicating that the larger outer chains are exclusively located on the Manα1→6 side. To calculate the exact amount of minor component with an exposed *N*-acetylglucosamine residue, fraction j was digested with jack bean β-*N*-acetylhexosaminidase. The result indicated that one *N*-acetyl-

Table III: Characteristics of Neutral Sugar Chains of Porcine ZP Glycoproteins

	without repeating[a]		with repeating		
	complete	incomplete[b]	complete	incomplete[b]	total of each rank
biantennary	22.8[c] (k1)[d]	18.3 (k2, l, m)	5.1 (j1)	0.8 (j2)	47.0
2,4-branched triantennary	10.7 (e1)	5.8 (a2, e2)	6.1 (g2, h2)	1.5 (g2)	24.1
2,6-branched triantennary	3.4 (i1)	6.0 (a3, b, c, i2)	3.0 (g3, h3)	1.4 (g3)	13.8
tetraantennary	3.5 (h1)	0.8 (a1)	3.6 (g1, f1, f2)	4.2 (d, g1, f1, f2)	12.1
total of each column	40.4	30.9	17.8	7.9	97.0

[a] *N*-Acetyllactosamine repeating units. [b] Oligosaccharides with exposed *N*-acetylglucosamine residues. [c] Percent molar ratio to the total neutral oligosaccharides. [d] Fractions of oligosaccharides in Table II are indicated in parentheses.

glucosamine residue was removed from 14% of fraction j (data not shown). On the basis of these results, the structures of fraction j are proposed, shown as j1 and j2 in Table II.

Fraction k was eluted at the position corresponding to that of authentic Gal_2·$GlcNAc_2$·Man_3·GlcNAc·Fuc·$GlcNAc_{OT}$ with a shoulder (Figure 3D). Diplococcal β-galactosidase digestion of fraction k produced a major radioactive peak with release of two galactose residues from the major peak and one from the shoulder (Figure 7D). By the subsequent digestion with diplococcal β-*N*-acetyhexosaminidase, this peak was converted to the fucosylated trimannosyl core with release of two *N*-acetylglucosamine residues (data not shown). These results indicate that Gal_2·$GlcNAc_2$·Man_3·GlcNAc·Fuc·$GlcNAc_{OT}$ (k1) and Gal·$GlcNAc_2$·Man_3·GlcNAc·Fuc·$GlcNAc_{OT}$ (k2) are included in this fraction. When fraction k was incubated with jack bean β-*N*-acetylhexosaminidase, one *N*-acetylhexosamine residue was released from the shoulder, yielding a smaller radioactive peak (Figure 7E). Since one mannose residue was released from the smaller peak by *A. saitoi* α-mannosidase II (data not shown), the exposed *N*-acetylglucosamine residue in k2 should be located on the Manα1→3 side. The proposed structures of k1 and k2 are shown in Table II.

Be sequential digestion with diplococcal β-galactosidase and diplococcal β-*N*-acetylhexosaminidase, fraction l was converted to the fucosylated trimannosyl core with release of one galactose residue and two *N*-acetylglucosamine residues (data not shown). Removal of one exposed *N*-acetylglucosamine residue from fraction l by jack bean β-*N*-acetylhexosaminidase (Figure 7F) followed by *A. saitoi* α-mannosidase II digestion resulted in no release of mannose residue. The data indicate that the oligosaccharide in fraction l has the isomeric structure of k2 as described above, in which the exposed *N*-acetylglucosamine residue is located at the Manα1→6 side (Table II).

Fraction m was converted to the fucosylated trimannosyl core with release of two *N*-acetylglucosamine residues by diplococcal β-*N*-acetylhexosaminidase digestion (data not shown). Therefore, degalactosylated biantennary structure is proposed for fraction m (Table II).

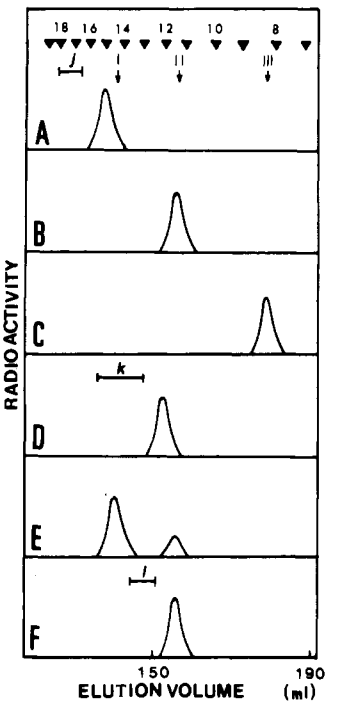

FIGURE 7: Sequential glycosidase digestions of oligosaccharides in Con A^+ and Con A^{++} fractions. Fraction j in Fig. 3D was sequentially digested with diplococcal β-galactosidase (panel A) and diplococcal β-*N*-acetylhexosaminidase (panel B). The radioactive peak in panel B was further subjected to another cycle of digestion with diplococcal β-galactosidase and diplococcal β-*N*-acetylhexosaminidase (panel C). Fraction k in Figure 3D was digested with diplococcal β-galactosidase (panel D). Fraction k was also digested with jack bean β-*N*-acetylhexosaminidase (panel E). Fraction l in Figure 3E was digested with diplococcal β-*N*-acetylhexosaminidase (panel F). Arrows indicate the elution positions of authentic oligosaccharides: I, Gal_2·$GlcNAc_2$·Man_3·GlcNAc·Fuc·$GlcNAc_{OT}$; II, Gal·GlcNAc·Man_3·GlcNAc·Fuc·$GlcNAc_{OT}$; III, Man_3·GlcNAc·Fuc·$GlcNAc_{OT}$. Black arrowheads are the same as in Figure 3. Bars j, k, and l in panels A, D, and F indicate the elution positions of fractions j, k, and l, respectively (see also Figure 3D,E).

Discussion

In the present study, structures of the N-linked neutral sugar chains of porcine ZP glycoproteins were investigated. Through this work, the structures of 31 oligosaccharides were elucidated, and several structural characteristics of the sugar moieties of these glycoproteins became evident. The sugar chains were found to be composed of a variety of complex-type oligosaccharides. Neither high mannose type nor hybrid-type oligosaccharide was detected. This result is compatible with the observation by Greve et al. (1982) that mouse ZP glycoproteins are sensitive to endo-β-*N*-acetylglucosaminidase F, but resistant to endo-β-*N*-acetylglucosaminidase H digestion. The in vitro biosynthetic study using growing mouse oocytes showed that high mannose type oligosaccharides of nascent ZP glycoproteins are processed to complex-type oligosaccharides in the Golgi. Therefore, the absence of high mannose type oligosaccharides in the mature form of mouse and porcine ZP glycoproteins indicates that a set of glycosyltransferases and processing enzymes leading to the formation of complex-type sugar chains are well expressed in the growing oocytes of both species.

Complex-type oligosaccharides found in porcine ZP glycoproteins are almost all fucosylated at their trimannosyl cores. However, several variations are observed in their outer chain moieties as summarized in Table III. First, biantennary, 2,4-branched and 2,6-branched triantennary, and tetraantennary oligosaccharides are included in an approximate molar ratio of 4:2:1:1. Second, 26% of these oligosaccharides contain *N*-acetyllactosamine repeating units in their outer chain moieties. The repeating sequences are all linear, and the extent of repeat is at most three times: $(Gal\beta1\rightarrow4GlcNAc\beta1\rightarrow3)_3$. This is quite different from mouse embryoglycans (Kamada

et al., 1987) which contain highly branched and elongated *N*-acetyllactosamine repeating units. Third, exposed *N*-acetylglucosamine residues partly occur in nonrepeating and repeating outer chain moieties of the oligosaccharides. These incompletely galactosylated oligosaccharides accounted for 39% of the total neutral oligosaccharides. This might be explained by the lower expression of galactosyltransferases in growing oocytes producing ZP glycoproteins. Other possibilities are also considered. Harpaz and Schachter (1980) reported that addition of bisecting *N*-acetylglucosamine to asparagine-linked sugar chains inhibits the processing of the sugar chains in the Golgi membrane. However, this is not the case, since no bisecting oligosaccharide was detected in the oligosaccharides reported here. It is also suspected that degalactosylation might result from the action of endogenous β-galactosidase during the purification procedure of ZP glycoproteins. To rule out this possibility, the oligosaccharide mixture released by hydrazinolysis of ZP glycoproteins, the galactose residues of which were labeled by the galactose oxidase–NaB^3H_4 method (Morell & Ashwell, 1972), was incubated with ovarian follicular fluid containing follicular cells and oocytes with vigorous stirring under the same conditions as used for purification of the ZP. Then, the supernatant was applied to a Bio-Gel P-2 column. The results indicated no release of radioactive galactose residue (data not shown). Therefore, it can be concluded that the occurrence of nongalactosylated *N*-acetylglucosamine residues in the outer chain moieties is an inherent characteristic of sugar chains of porcine ZP glycoproteins.

Several lines of evidence suggest that the sugar moieties of ZP glycoproteins play a role in the interaction of mammalian sperm with eggs at the inital stage of fertilization. One of the well-studied examples is that O-linked oligosaccharides with α-linked galactose residues of mouse egg ZP3 have a sperm receptor activity (Florman & Wassarman, 1985; Bleil & Wassarman, 1988). It has also been suggested that galactosyltransferase located on plasma membrane of the mouse sperm head mediates the binding of sperm to eggs (Shur & Hall, 1982; Lopez et al., 1985; Shur & Neely, 1988). In this context, certain oligosaccharides with exposed *N*-acetylglucosamine residues might be recognized as acceptors for the enzyme, although their structures have not been elucidated in the mouse system. Interestingly, the present study showed that considerable quantities of N-linked, neutral oligosaccharides in porcine ZP glycoproteins are terminated with *N*-acetylglucosamine residues. Our preliminary observation that α-lactalbumin, an inhibitor of galactosylation of *N*-acetylglucosamine by galactosyltransferase, inhibits the binding of boar sperm to its eggs (data not shown) may indicate that exposed *N*-acetylglucosamine residues in the oligosaccharides serve at least as one of the sperm binding determinants in the porcine system. Of interest also is the occurrence of lectin-like proteins on boar sperm which bind to fucose (Topfer-Petersen et al., 1985). Whether fucosyl residues found in almost all of the neutral oligosaccharides are recognized by the sperm lectin is a subject to be investigated in the future.

It is known that sperm are loosely attached to the ZP immediately after mixing with eggs and then the attached sperm bind more tightly to ZP. The bound sperm undergo the acrosome reaction, by which the inner acrosome membrane of sperm is exposed, penetrates the ZP, and finally fuses with egg plasma membrane (Wassarman, 1987; Yanagimachi, 1988). Thus, the sperm–egg interaction is very complicated. It is quite possible that multiple recognition mechanisms are involved in these processes. As discussed above, the present study on the N-linked, neutral oligosaccharides provided interesting structural aspects for the elucidation of proposed roles of the sugar moieties of ZP glycoproteins in the sperm–egg interaction. Analysis of N-linked, acidic oligosaccharides is currently immature but suggests that these oligosaccharides are sulfated (data not shown). This characteristic is also notable in view of the fact that sulfated glycans such as dextran sulfate and fucoidin inhibit the binding of sperm to egg in several mammalian species including pig (Huang & Yanagimachi, 1984; Jones et al., 1988). Thus detailed analysis of the sugar moieties of ZP glycoproteins will help us to find a clue to the understanding of molecular mechanism of fertilization.

Acknowledgments

We express our gratitude to Ms. Yumiko Kimizuka and Ms. Tamae Takahashi for their secretarial assistance.

References

Amano, J., & Kobata, A. (1986) *J. Biochem. (Tokyo) 99*, 1645–1654.
Bleil, J. D., & Wassarman, P. M. (1980a) *Cell 20*, 873–883.
Bleil, J. D., & Wassarman, P. M. (1980b) *Dev. Biol. 76*, 185–203.
Bleil, J. D., & Wassarman, P. M. (1988) *Proc. Natl. Acad. Sci. U.S.A. 85*, 6778–6782.
Cummings, R. D., & Kornfeld, S. (1982) *J. Biol. Chem. 257*, 11235–11240.
Cummings, R. D., & Kornfeld, S. (1984) *J. Biol. Chem. 259*, 6253–6260.
Dumbar, B. S., Wardrip, N. J., & Hedrick, J. L. (1980) *Biochemistry 19*, 356–365.
Florman, H. M., & Wassarman, P. M. (1985) *Cell 41*, 313–324.
Glasgow, L. R., Paulson, J. C., & Hill, R. L. (1977) *J. Biol. Chem. 252*, 8615–8623.
Greve, J. M., Salzmann, G. S., Roller, R. J., & Wassarman, P. M. (1982) *Cell 31*, 749–759.
Gwatkin, R. B. L. (1977) in *Fertilization Mechanisms in Man and Mammals*, Plenum, New York.
Harpaz, N., & Schachter, H. (1980) *J. Biol. Chem. 255*, 4894–4902.
Hedrick, J. L., & Wardrip, N. J. (1987) *Dev. Biol. 121*, 478–488.
Huang, T. T. F., & Yanagimachi, R. (1984) *Exp. Cell Res. 153*, 363–373.
Jones, R., Brown, C. R., & Lancaster, R. T. (1988) *Development 102*, 781–792.
Kagawa, Y., Takasaki, S., Utsumi, J., Hosoi, K., Shimizu, H., Kochibe, N., & Kobata, A. (1988) *J. Biol. Chem. 263*, 17508–17515.
Kamada, Y., Arita, Y., Ogata, S., Muramatsu, H., & Muramatsu, T. (1987) *Eur. J. Biochem. 163*, 497–502.
Kitamikado, M., Ito, M., & Li, Y. T. (1982) *Methods Enzymol. 83*, 619–625.
Kohyama, K., Hasegawa, A., Tsuji, Y., & Isojima, S. (1985) *J. Reprod. Immunol. 3*, 147–156.
Li, Y. T., & Li, S. C. (1982) *Methods Enzymol. 28*, 702–713.
Lopez, L. C., Bayna, E. M., Litoff, D., Shaper, N. L., Shaper, J. H., & Shur, B. D. (1985) *J. Cell Biol. 101*, 1501–1510.
Mizoguchi, A., Takasaki, S., Maeda, S., & Kobata, A. (1984) *J. Biol. Chem. 259*, 11949–11957.
Morell, A. G., & Ashwell, G. (1972) *Methods Enzymol. 28*, 205–208.
Noda, Y., Mori, T., Takai, I., Kohda, H., & Nishimura, T. (1981) *J. Reprod. Immunol. 3*, 147–156.

Ohkura, T., Yamashita, K., Mishima, Y., & Kobata, A. (1984) *Arch. Biochem. Biophys. 235*, 63–77.
Ringuette, M. J., Sobieski, D. A., Chamow, S. M., & Dean, J. (1986) *Proc. Natl. Acad. Sci. U.S.A. 83*, 4341–4346.
Shimizu, S., Tsuji, M., & Dean, J. (1983) *J. Biol. Chem. 258*, 5858–5863.
Shur, B. D., & Hall, N. G. (1982) *J. Cell Biol. 95*, 574–579.
Shur, B. D., & Neely, A. G. (1988) *J. Biol. Chem. 263*, 17706–17714.
Stambaugh, R. (1978) *Gamete Res. 1*, 65–85.
Takasaki, S., Mizuochi, T., & Kobata, A. (1982) *Methods Enzymol. 83*, 263–268.
Takasaki, S., Murray, G. J., Furbish, F. S., Brady, R. O., Barranger, J. A., & Kobata, A. (1984) *J. Biol. Chem. 259*, 10112–10117.
Takeuchi, M., Takasaki, S., Miyazaki, H., Kato, T., Hoshi, S., Kochibe, N., & Kobata, A. (1988) *J. Biol. Chem. 263*, 3657–3663.
Topfer-Petersen, E., Friess, A. E., Nguyen, H., & Schill, W. B. (1985) *Histochemistry 83*, 139–145.
Wassarman, P. M. (1987) *Annu. Rev. Cell Biol. 3*, 109–142.
Wassarman, P. M., Florman, H. M., & Greve, J. M. (1985) in *Biology of Fertilization* (Metz, C. B., & Monroy, A. Eds.) Vol. 2, pp 341–360, Academic, New York.
Yamashita, K., Ohkura, T., Yoshima, H., & Kobata, A. (1981) *Biochem. Biophys. Res. Commun. 100*, 226–232.
Yamashita, K., Mizuochi, T., & Kobata, A. (1982) *Methods Enzymol. 83*, 105–126.
Yamashita, K., Kochibe, N., Ohkura, T., Ueda, I., & Kobata, A. (1985) *J. Biol. Chem. 260*, 4688–4693.
Yamashita, K., Totani, K., Ohkura, T., Takasaki, S., Goldstein, I. J., & Kobata, A. (1987) *J. Biol. Chem. 262*, 1602–1607.
Yanagimachi, R. (1988) in *The physiology of reproduction* (Knobil, E., & Neil, J. L., Eds.) Vol. 1, p 135, Raven, New York.
Yazawa, S., Furukawa, K., & Kochibe, N. (1984) *J. Biochem. (Tokyo) 96*, 1737–1742.
Yoshima, H., Takasaki, S., & Kobata, A. (1980) *J. Biol. Chem. 255*, 10793–10804.
Yurewicz, E. C., Sacco, A. G., & Subramanian, M. G. (1987) *J. Biol. Chem. 262*, 564–571.

High Channel-Mediated Water Permeability in Rabbit Erythrocytes: Characterization in Native Cells and Expression in *Xenopus* Oocytes†

Shih-Ting Tsai, Rubin Zhang, and A. S. Verkman*
Departments of Medicine and Physiology, Cardiovascular Research Institute, University of California, San Francisco, California 94143-0532

Received September 4, 1990; Revised Manuscript Received November 8, 1990

ABSTRACT: Erythrocytes from several mammalian species contain mercurial-sensitive water transporters. By a stopped-flow light scattering technique, osmotic water permeability (P_f) was exceptionally high in rabbit erythrocytes (0.053 ± 0.002 cm/s) and reversibly inhibited by 98% by *p*-(chloromercuri)benzenesulfonate (pCMBS). The activation energy (E_a) was 4.6 kcal/mol (15–37 °C). pCMBS inhibition was half-maximal at 0.1 mM (60-min incubation); at 1 mM pCMBS, half-maximal inhibition occurred in 8 min. P_f was also inhibited by $HgCl_2$ and pCMB with >90% inhibition in 5 min. There was no inhibition by high concentrations of phloretin, DNDS, cytochalasin B, amiloride, ouabain, furosemide, and several proteases. In defolliculated *Xenopus* oocytes microinjected with 50 nL of water or unfractionated mRNA (1 mg/mL) from rabbit reticulocytes, oocyte P_f assayed at 10 °C after 72-h incubation increased from (4 ± 1) × 10^{-4} cm/s (water injected) to (18 ± 2) × 10^{-4} cm/s (mRNA injected). P_f increased linearly with [mRNA] (0–75 ng/oocyte) and was inhibited slowly and reversibly by pCMBS and immediately by $HgCl_2$ but not by cytochalasin B, phloretin, or DNDS. E_a was 9.6 kcal/mol (water injected) and 2.6 kcal/mol (mRNA injected). These results demonstrate that rabbit erythrocytes have the highest P_f and the greatest percentage inhibition of P_f by mercurials of any mammalian erythrocyte studied. The characteristics of the expressed and native water channels were similar, suggesting that the erythrocyte water channel is a membrane protein suitable for expression cloning.

The water permeability of human erythrocytes has been the subject of considerable interest. From biophysical measurements, including (a) high osmotic water permeability (P_f = 0.02 cm/s), (b) a ratio of osmotic-to-diffusional water permeability (P_f/P_d) > 3, (c) a low activation energy (E_a = 4.5 kcal/mol), and (d) 90% inhibition of P_f by mercurials, it has been concluded that the erythrocyte contains a specialized pore or channel for facilitated water transport (Macey, 1984; Solomon et al., 1984). It was proposed that rapid water transport is important for protection of erythrocyte integrity during passage through and return from the hypertonic renal medulla (Macey, 1984).

The molecular identity of the erythrocyte water channel is uncertain. Studies of [^{203}Hg]pCMBS binding have raised the possibility that the anion transport protein band 3 is the water channel (Benga et al., 1986); however, the lack of water transport inhibition by anion transport inhibitors and the

†This work was supported by Grants DK35124, DK39354, and DK16095 from the National Institutes of Health and a grant from the National Cystic Fibrosis Foundation. S.-T.T. was supported by a student fellowship from the American Heart Association, Northern California Affiliate. A.S.V. is an Established Investigator of the American Heart Association.

*Address correspondence to this author at 1065 Health Sciences East Tower, Cardiovascular Research Institute, University of California, San Francisco, San Francisco, CA 94143-0532.

0006-2960/91/0430-2087$02.50/0